



TITLE:

Linear strain flows with and without boundaries : the regularizing effect of the pressure term (Turbulence Transport, Diffusion and Mixing)

AUTHOR(S):

Pelz, Richard B.; Ohkitani, Koji

CITATION:

Pelz, Richard B. ...[et al]. Linear strain flows with and without boundaries : the regularizing effect of the pressure term (Turbulence Transport, Diffusion and Mixing). 数理解析研究所講究録 2003, 1339: 230-241

ISSUE DATE:

2003-09

URL:

<http://hdl.handle.net/2433/43444>

RIGHT:

Linear strain flows with and without boundaries —the regularizing effect of the pressure term—

Rutgers University R.B. Pelz(deceased)[18] · 京大数理研 大木谷 耕司

I. INTRODUCTION

In this work a flow developing from the linear straining flow,

$$(u_0, v_0, w_0) = -(y + z, z + x, x + y),$$

and a flow whose initial condition is locally similar to it, namely,

$$\mathbf{u} = -(\sin y + \sin z, \sin z + \sin x, \sin x + \sin y)$$

is examined. The linear straining flow is not in $L^2(\mathbb{R}^3)$ (energy is not bounded), it is boundary-free (no conditions are imposed at infinity) and it has non-unique solutions, some of which blow up in finite time, e.g.

$$\mathbf{u}(x, y, z, t) = \left(\frac{y+z}{t-1}, \frac{z+x}{t-1}, \frac{x+y}{t-1} \right),$$

$$p(x, y, z, t) = -\frac{x^2 + y^2 + z^2}{(t-1)^2}.$$

The latter flows match the linear flow to first order at the origin, but are in $L^2(\mathbb{T}^3)$ and have outer boundary conditions. It is found in this work through numerical simulations of these flows, that the latter flow solutions remain smooth at least for a time well beyond the critical time of the linear flow. The overall goal is to explore whether or not a finite-energy solution to the Euler equations of hydrodynamics can blow up in finite time. The immediate goal is to understand the difference in these two types of flows, how outer boundary conditions affect the solution near the origin, and in particular what the role of pressure is. An answer to the latter question may shed some light on the first.

If the diagonal transformation, defined as $\mathbf{x} = \mathbf{A}\mathbf{x}'$, $\mathbf{u}'(\mathbf{x}') = \mathbf{A}^T \mathbf{u}(\mathbf{A}\mathbf{x}')$ with

$$\mathbf{A} = \begin{pmatrix} 1/\sqrt{2} & 1/\sqrt{6} & 1/\sqrt{3} \\ -1/\sqrt{2} & 1/\sqrt{6} & 1/\sqrt{3} \\ 0 & -2/\sqrt{6} & 1/\sqrt{3} \end{pmatrix},$$

is used, the straining flow is written

$$(u'_0, v'_0, w'_0) = (x', y', -2z')$$

and the strain rate matrix, $S_{i,j} = 1/2(\partial u_i/\partial x_j + \partial u_j/\partial x_i)$, is $S_0 = \text{diag}(1, 1, -2)$ initially, that is,

$$S_0 = \begin{pmatrix} 0 & -1 & -1 \\ -1 & 0 & -1 \\ -1 & -1 & 0 \end{pmatrix} \rightarrow A^T S_0 A = \begin{pmatrix} 1 & 0 & 0 \\ 0 & 1 & 0 \\ 0 & 0 & -2 \end{pmatrix}$$

A number of such boundary-free fields have exact solutions to the Euler and Navier-Stokes equations and have been examined by [1–9]. They are especially interesting because of their blowup behavior.

Since the linear straining flow is not in $L_2(\mathbb{R}^3)$, it should be considered as a flow local to the origin. Realizing this, Bhattacharjee *et al.* examined a number of flows, and found under certain conditions the local flow solution possessed a finite-time singularity [7, 8]. There was not a way, however, to consistently account for outer boundary conditions. In the present work, the opposite approach is taken, that is, a number of specific flows with local behavior being the linear flow but with *bona fide* outer conditions are examined.

II. LINEAR STRAIN FLOW

To describe the behavior of the sine flow around the origin, we fix notations (by Bhattacharjee *et al.*) as follows. We consider the Taylor expansions around the origin;

$$u(x, y, z) = b(t)(y + z) + O(|\mathbf{x}|^3),$$

$$p(x, y, z) = -d(t)(x^2 + y^2 + z^2) - e(t)(xy + yz + zx) + O(|\mathbf{x}|^4),$$

where three functions of t for the local description have been introduced

$$b(t) = \left. \frac{\partial u}{\partial y} \right|_{\mathbf{x}=0}, \quad d(t) = -\left. \frac{1}{2} \frac{\partial^2 p}{\partial x^2} \right|_{\mathbf{x}=0}, \quad e(t) = -\left. \frac{\partial^2 p}{\partial x \partial y} \right|_{\mathbf{x}=0}.$$

Other components of velocity are obtained by cyclic permutations.

The linear straining flow solution can be examined as a special exact solution of the strain-rate equation, e.g. by Majda's construction [9].

Below $\omega(t)$, $S(t)$, $P(t)$ are spatially uniform vorticity, strain rate and pressure hessian, respectively.

For an arbitrarily given $S(t)$, let us solve

$$\frac{d\omega}{dt} = S(t)\omega(t).$$

and define

$$P(t) \equiv -\frac{dS}{dt} - S^2 - \frac{\omega \otimes \omega - |\omega|^2 I}{4}.$$

If we form

$$u(x, t) = \frac{1}{2}\omega(t) \times x + S(t)x,$$

$$p(x, t) = \frac{1}{2}P_{ij}x_i x_j$$

then the pair (u, p) solves the Euler equations.

For the case under consideration we have $\omega = 0$ and

$$S = \begin{pmatrix} 0 & b(t) & b(t) \\ b(t) & 0 & b(t) \\ b(t) & b(t) & 0 \end{pmatrix},$$

so the pressure hessian becomes

$$P = - \begin{pmatrix} 2b(t)^2 & b'(t) + b(t)^2 & b'(t) + b(t)^2 \\ b'(t) + b(t)^2 & 2b(t)^2 & b'(t) + b(t)^2 \\ b'(t) + b(t)^2 & b'(t) + b(t)^2 & 2b(t)^2 \end{pmatrix} = - \begin{pmatrix} 2d(t) & e(t) & e(t) \\ e(t) & 2d(t) & e(t) \\ e(t) & e(t) & 2d(t) \end{pmatrix},$$

where the definitions of $d(t)$, $e(t)$ have been used in the final equality. Thus we find for our case

$$\frac{d}{dt}b(t) + b(t)^2 = e(t),$$

$$d(t) \equiv b(t)^2$$

The problem can be viewed as follows; for a given $e(t)$, the solution $b(t)$ can be found by solving the Ricatti equation $b'(t) = -b(t)^2 + e(t)$. Note that the pressure Hessian can be written as

$$P = \frac{\Delta p}{3}I - \begin{pmatrix} 0 & e(t) & e(t) \\ e(t) & 0 & e(t) \\ e(t) & e(t) & 0 \end{pmatrix}$$

where I denotes the identity matrix. The eigenvalues of the second (non-local) term of P are $(-e(t), -e(t), 2e(t))$.

A solution can be found in which the Hessian is isotropic. Setting $e(t) \equiv 0$, the Ricatti equation $b'(t) = -b(t)^2$ has the solution

$$b(t) = \frac{b(0)}{1 + b(0)t}, \quad (b(0) = -1)$$

This solution is the one that is selected as an example of blowup. It has isotropic pressure Hessian in the sense that $P = \frac{I}{3}\Delta p$. This model is known as the Restricted Euler Equations and they have blowup solutions [11–16].

A nonzero $e(t)$ does not necessarily mean the solution does not blow up. If $e(t)$ has the form $\alpha b(t)^2$, where $0 < \alpha < 1$. The solution is

$$b(t) = \frac{1}{1 + b_0(1 - \alpha)t},$$

which simply delays blowup to a time $1/[|b_0|(1 - \alpha)]$.

In order to desingularize the solution, the growth in $e(t)$ must be stronger than $b(t)^2$. If $e(t)$ has the form

$$e(t) = \beta(|b(0)|t)^\alpha b(t)^2, \quad \alpha > 0$$

for $\alpha > 0$, then the solution is

$$b(t) = \frac{b(0)}{1 + b(0)t \left(1 - \frac{\beta(|b(0)|t)^\alpha}{\alpha+1}\right)}.$$

For example, it is readily seen that with $\alpha = 1$ this is regular for $\beta > 1/2$.

Clearly, the arbitrariness of $e(t)$ is the origin of the non-uniqueness of solutions. In this formulation, however, the physical nature of $e(t)$ is missing.

III. THE SERIES SOLUTION

Some understanding of the solution with isotropic Hessian is gained by examining the time power series solution. If a power series in time is assumed

$$u = \sum_{k=0}^{\infty} u_k t^k$$

then each term can be found in the following three steps

$$\tilde{u} = - \sum_{k=0}^{n-1} u_k \cdot \nabla u_{n-k-1}, \quad \Delta p = \nabla \cdot \tilde{u}, \quad u_n = (\tilde{u} - \nabla p)/n.$$

Let $u_0 = (x', y', -2z')$ be the linear straining flow. In the first stage of computing u_1 , \tilde{u} is $-(x', y', 4z')$ (the diagonal frame is assumed). The pressure equation is then $\Delta' p = -6$. If the particular solution is taken, $p = -(x'^2 + y'^2 + z'^2)$, the result is

$$u_1 = u_0.$$

In fact, using the same particular solution, each subsequent term is u_0 and so

$$u = u_0(1 + t + t^2 + \dots) = \frac{u_0}{1-t}.$$

The particular blowup solution with isotropic pressure Hessian given in the previous section, is the same as the series solution where only the particular solution to the pressure Poisson problem is selected.

The homogeneous solution, which allows the general solution to satisfy boundary conditions, cannot be constructed in this boundary-free flow.

In addition, the constant right-hand-side of the pressure Poisson equation is a solution to Laplace's equation. While valid only for solutions in L_2 , the Fredholm Alternative for $L\phi = f$ states that if the differential operator, L is singular, f must be orthogonal to the space of homogeneous solution in order for L_2 solutions to exist. If the right-hand-side is not orthogonal, secular behavior is expected.

When such a resonance behavior develops in regular perturbation problems, the secular term limits the convergence of the perturbation series solution. When proper homogeneous solutions are included and the series is summed, or a method of multiple scales is used, the correct behavior is recovered. Both methods rely, however, on specific boundary conditions given.

IV. NUMERICAL RESULTS

A group of incompressible flows that have the D_{3d} symmetry in a unit cell and are embedded in a cubic lattice can be defined [10]. These flows are then in the domain T^3 , have periodic boundary conditions and can be represented by Fourier series in space. The sine flow

is one such example and was investigated by Childress and Spiegel (private communication, see also [17]).

To first order around the origin, the sine flow is equivalent to the linear straining flow. As with all the flows considered, the Riccati equation $b'(t) = -b(t)^2 + e(t)$, where $b(t)$ is $\partial u / \partial y$ holds at the origin. In this case, $e(t)$ is generated consistently with the evolution of the complete flow. The sine flow, hence, provides an example of a local linear-straining flow with outer boundary conditions.

The initial value problem – Euler equations for incompressible flow with periodic boundary conditions and sine initial condition – was solved by two methods: a Fourier pseudo-spectral method and a power series in time.

A standard Fourier spectral method was employed to solve the Euler equations. Aliasing errors were removed by the 2/3 rule, so the maximum wavenumber is $N/3$ for calculations with N^3 grid points. Typically, we use $N = 256$. A symmetry has been used for reducing memory size and calculation amount. Time-marching was performed by 4th order Runge-Kutta scheme with a typical time increment $\Delta t = 2.5 \times 10^{-3}$.

The recursion for the n -th term in the power series can be written

$$\mathbf{u}_n = -\frac{1}{n}(\mathbf{I} - \nabla \Delta^{-1} \nabla \cdot) \sum_{k=0}^{n-1} (\mathbf{u}_k \cdot \nabla) \mathbf{u}_{n-k-1}$$

Maple was used to find the first 20 terms of the series with the Fourier coefficients as rational numbers (exact precision).

Figure Fig.1 shows the evolution of $b(t)$, where we compare the pseudo-spectral solution and the series solution. It is clear that the sine flow departs quickly from the singular behavior of the linear strain flow. Moreover after $t = 1$ where the the linear strain flow blows up, the strain $b(t)$ starts decreasing in magnitude. The numerical accuracy was checked at $t = 2$ by examining the exponential fall-off the energy spectrum. The series solution and its Padé approximation agree well with the spectral result up to times $t = 0.9$ and 1.5 , respectively. Therefore this numerical result shows that the sine flow remains regular at least for a time well beyond the critical time of the linear flow.

This indicates that off-diagonal element of the pressure hessian $e(t)$ plays an important role. In Fig.2 we show the time evolution of $e(t)$. As expected, $e(t)$ grows in time to quench the growth of $b(t)$. This behavior of $e(t)$ shows that the assumption of isotropic pressure hessian does not persist in time under the Eulerian dynamics with appropriate boundary

conditions. Apparently $e(t)$ grows so fast that the singularity of $b(t)$ corresponding to the linear strain flow is desingularized, or at least delayed. In order to quantify how fast $e(t)$ increases in comparison with $b(t)$ we show the nondimensional ratio $e(t)/b(t)^2$ in Fig.3. It is remarkable that the ratio shows a clear straight line up to $t = 1$ with the slope close to 1. As noted above $e(t) = k(|b(0)|t)^\alpha b(t)^2$ with $\alpha = 1$, $k > 1/2$ is regular all time, consistent with the numerical result. At present there is no explanation why the ratio behaves linearly in time.

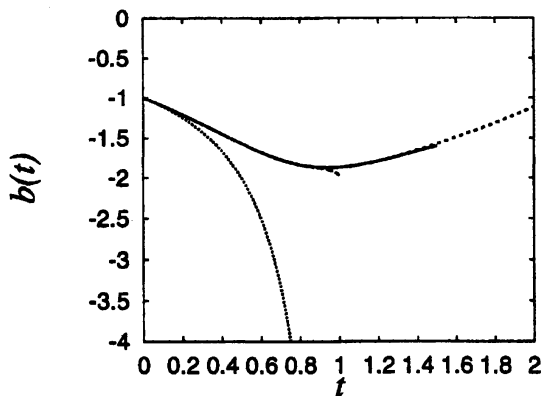


FIG. 1: Time evolution of $b(t)$; spectral(solid), the 20-term series (short-dashed), the [10,10] Padé (long-dashed) and $1/(1-t)$ (dotted).

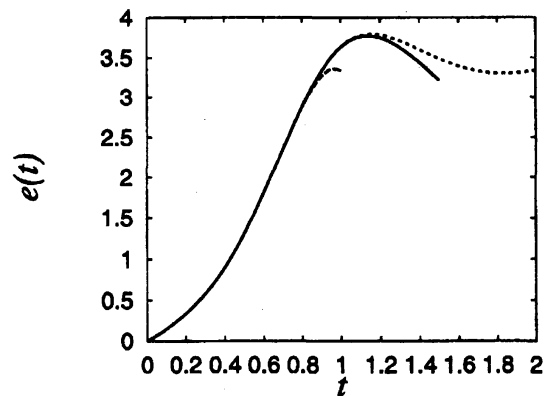


FIG. 2: Time evolutions of $e(t)$; spectral(solid), the 20-term series (short-dashed) and the [10,10] Padé (long-dashed).

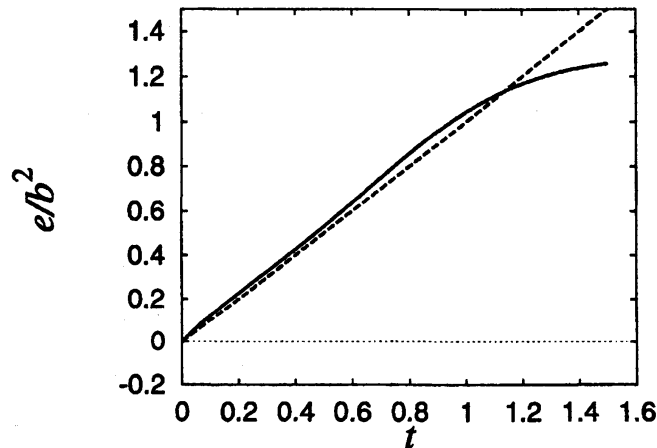


FIG. 3: Time evolution of $e(t)/b(t)^2$. The dotted line is t .

V. HIGHER-ORDER 'RAMP' APPROXIMATION

Next we seek a better way of approximating the linear strain flow under periodic boundary conditions. The sine flow behaves like the linear strain flow to leading order with an error of $O(x^3)$ near the origin. We can make the error smaller by choosing a linear combination of sine's appropriately as follows. Consider a function, which will be called a 'ramp' function,

$$\begin{aligned} r_n(x) &= \sum_{p=1}^n a_p \sin(px) \\ &= \left(\sum_{p=1}^n p a_p \right) x - \left(\frac{1}{3!} \sum_{p=1}^n p^3 a_p \right) x^3 + \dots \end{aligned}$$

Requiring that

$$r_n(x) = x + O(x^{2n+1})$$

we find

$$\sum_{p=1}^n p a_p = 1, \quad \sum_{p=1}^n p^k a_p = 0 \text{ for } k = 2, \dots, n.$$

In terms of determinants a formula for general coefficients is obtained as

$$a_p = \frac{\begin{vmatrix} 0 & 0 & \dots & 1 & \dots & 0 \\ 1 & 2^3 & \dots & p^3 & \dots & n^3 \\ \dots & \dots & \dots & \dots & \dots & \dots \\ 1 & 2^{2n-1} & \dots & p^{2n-1} & \dots & n^{2n-1} \end{vmatrix}}{\begin{vmatrix} 1 & 2 & \dots & p & \dots & n \\ 1 & 2^3 & \dots & p^3 & \dots & n^3 \\ \dots & \dots & \dots & \dots & \dots & \dots \\ 1 & 2^{2n-1} & \dots & p^{2n-1} & \dots & n^{2n-1} \end{vmatrix}}, \quad (p = 1, 2, \dots, n).$$

The first few approximations are

$$\begin{aligned} r_1(x) &= \sin x, \\ r_2(x) &= \frac{4}{3} \sin x - \frac{1}{6} \sin 2x, \\ r_3(x) &= \frac{3}{2} \sin x - \frac{3}{10} \sin 2x + \frac{1}{30} \sin 3x, \\ r_4(x) &= \frac{8}{5} \sin x - \frac{2}{5} \sin 2x + \frac{8}{105} \sin 3x - \frac{1}{140} \sin 4x. \end{aligned}$$

We have performed pseudo-spectral computations using $r_n(x)$ as initial condition ($n = 2, 3, \dots, 10$). We show the time evolution of $b(t)$ for them in Fig.4. As the order of approximation n is increased, $|b(t)|$ increases more rapidly than the sine flow ($n = 1$). With $n = 3$ it behaves quite similar to the linear strain flow up to $t = 0.6$. However, with $n \geq 4$, $|b(t)|$ overshoots the linear strain flow, without no hint of convergence toward it.

The strain rate $b(0) = -1$ at the origin sets a local time scale. The higher the order of approximation is, the wider the region extends where a good agreement is reached between the linear strain flow and the approximations. The departure observed above not only the local time scale but some global time scale is important for long time evolution. It is not surprising that we need a global time scale to compare the behavior of higher-order approximations with that of the linear strain flow.

As a trial we choose here a time scale defined by a global strain rate

$$\tau = t \|S\|_{L^2}.$$

(Remember that the linear strain flow is irrotational.) For the linear strain flow, we have $\|S\|_{L^2} = \sqrt{6}$. For the higher-order approximations we have

$$\|S\|_{L^2} = \left(\frac{1}{(2\pi)^3} \int S_{ij} S_{ij} dx \right)^{1/2} = \left(\frac{1}{(2\pi)^3} \int \frac{|\omega|^2}{2} dx \right)^{1/2}.$$

So we can compare them directly. Such a comparison of $b(t)$ is made in Fig.5.

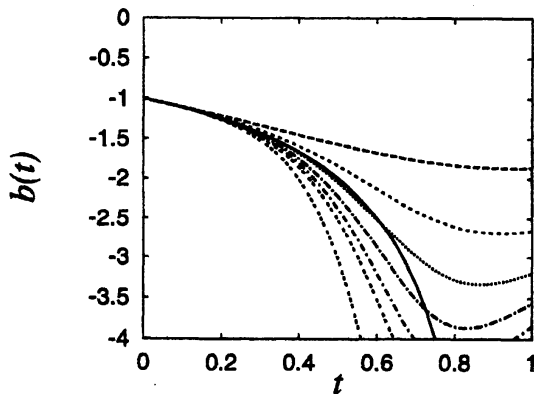


FIG. 4: Time evolution of $b(t)$ for the approximations of order $n = 1, 2, 3, 4, 5, 6, 10$ (long-dashed, dashed, dotted, dot-dashed, dot-short-dashed, 2-dashed and 3-dashed). The solid line is for $1/(t-1)$.

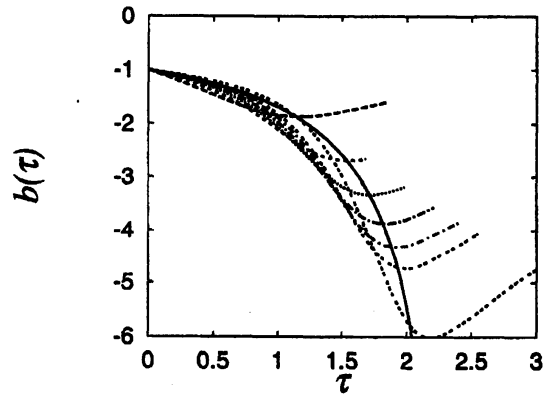


FIG. 5: Time evolution of $b(\tau)$ scaled by the global strain rate, for the approximations of order $n = 1, 2, 3, 4, 5, 6, 10$ (long-dashed, dashed, dotted, dot-dashed, dot-short-dashed, 2-dashed and 3-dashed). The solid line is for $1/(\tau/\sqrt{6} - 1)$.

The time evolution when scaled by the global strain rate, appears a little bit more singular than the linear strain flow but the approximations have a trend of approaching to it. To check the time dependence of $b(\tau)$ we plot $-1/b(\tau)$ in Fig.6.

It is of interest to see how $e(\tau)$ behaves we plot it in Fig.7. It should be noted that for $n \geq 3$ and notably for $n \geq 4$ in particular, $e(\tau)$ becomes negative for some time intervals and are positive again later. This means that it enhances the growth of $|b(t)|$ for those time intervals.

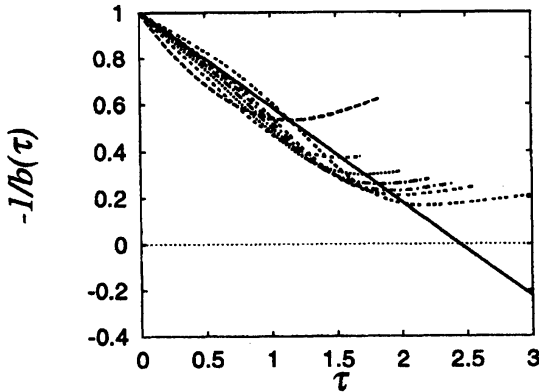


FIG. 6: Time evolution of $-1/b(\tau)$, plotted as in Fig.5. The solid line is for $1 - \tau/\sqrt{6}$.

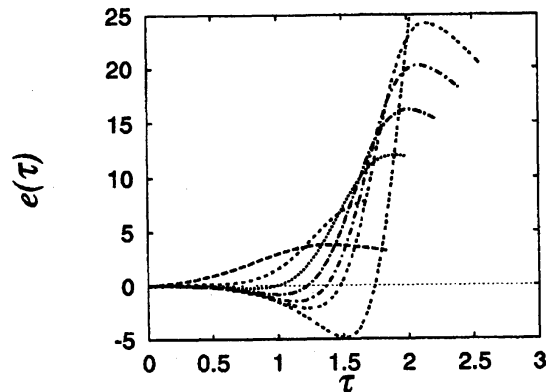


FIG. 7: Time evolution of $e(\tau)$, plotted as in Fig.6.

VI. SUMMARY AND OUTLOOK

We have performed numerical simulations of the sine flow, which is similar to the linear strain flow at the origin. It is shown that the off-diagonal elements of the pressure hessian grows so fast in the sense that $(b(0) = -1)$

$$e(t) = \beta t b(t)^2, \quad (\beta > 1).$$

As a result, the blowup seen in the latter flow is removed, or at least delayed. Numerical simulations of higher-order ramp approximations have also been performed to mimic the linear strain flow more faithfully than the sine flow. A trend was seen for them to approach the latter.

On the basis of the Taylor series expansion, we see that the non-uniqueness of the linear strain flow stems from arbitrariness of the homogeneous solutions to the Poisson equation. In an analogy with singular perturbation problems, it may be useful to take into

account the outer boundary conditions implicitly by introducing the a homogeneous term of the same order. It may be useful to study how the complex singularities in t move away from the real time axis. Details on these issues will be reported elsewhere.

Acknowledgments

この研究は Pelz 氏が 2002 年 5 月から 8 月まで、客員教授として数理解析研究所に滞在した際に行われた。

-
- [1] HOPF, E. 1952 Statistical hydromechanics and functional calculus *J. Rat. Mech. Anal.* **1** 87–123.
 - [2] OKAMOTO, H 1994 A uniqueness theorem for the unbounded classical solution of the nonstationary Navier-Stokes equations in \mathcal{R}^3 . *J. Math. Anal. Appl.* **181** 473–482.
 - [3] CHILDRESS, S., IERLEY, G.R., SPIEGEL, E.A. & YOUNG, W.R. 1989 Blow-up of unsteady two-dimensional Euler and Navier-Stokes solutions having stagnation-point form. *J. Fluid Mech.* **203** 1–22.
 - [4] OHKITANI, K. 1990 A class of simple blow-up solutions with uniform vorticity to three dimensional Euler equations. *J. Phys. Soc Japan* **59** 3811–3814.
 - [5] CHEN, X. AND OKAMOTO, H. 2000 Global existence of solutions to the Proudman-Johnson equation. *Proc. Jpn. Acad.* **76 A** 149–152.
 - [6] CHILDRESS, S. 2001 Euler singularities from the Lagrangian viewpoint. in *An Introduction to the Geometry and Topology of Fluid Flows*, R.L.Ricca, ed., IUTAM Symposium Series, Kluwer 2001, 313–328.
 - [7] BHATTACHARJEE, A.& WANG, X. 1992 Finite time vortex singularity in a model of three-dimensional Euler flows. *Phys. Rev. Lett.* **69** 2196–2200.
 - [8] BHATTACHARJEE, A., NG, C.S.& WANG, X. 1995 Finite-time vortex singularity and Kolmogorov spectrum in a symmetric three-dimensional spiral model. *Phys. Rev. E* **52** 5110–5123.
 - [9] MAJDA, A. 1986 Vorticity and the mathematical theory of incompressible fluid flow. *Comm. Pure Appl. Math.* **39** 187–220.

- [10] PELZ, R.B. 2002 Discrete groups, symmetric flows and hydrodynamic blowup. in *Tubes, sheets and singularities in Fluid Dynamics*, K.Bajer, ed., IUTAM Symposium Series, Kluwer 2002,
- [11] LEORAT, J. 1975 La turbulence megnetohydrodynamique helicitaire et la generation des champs magnetique a grande echelle. PhD thesis submitted to L'Uinversite de Paris VII, Appendix A4.
- [12] VIEILLEFOSSE, P. 1982 Local interaction between vorticity and shear in a incompressible flow. *J. Phys.(Paris)***43** 837-842.
- [13] VIEILLEFOSSE, P. 1984 Internal motion of a small element of an inviscid flow. *Physical***125A** 150-162.
- [14] NOVIKOV, E.A. 1990 Internal dynamics of flows and formation of singularities. *Fluid Dyn. Res.***6** 79-89.
- [15] CANTWELL, B.J. 1992 Exact solution of a restricted Euler equation for the velocity gradient tensor. *Phys. Fluids.A* **4** 461-160.
- [16] TADMOR, E. 2002 Spectral dynamics of the velocity gradient field in restricted flows. *Commun. Math. Phys.***228** 435-466.
- [17] ROSE, H.A. & SULEM, P.L. Fully developed turbulence and statistical mechanics. *J. Phys.(Paris)***39** 441-484.
- [18] 2002 年 9 月に亡くなられた Pelz 氏との共同研究に関するこの原稿は、彼の書き残したドラフトを大木谷が大幅に編集・修正した上で英語で書いたものである。編集を全く施していない彼の遺稿は、別の講究録 1326 「流体力学における Rich Pelz の貢献」中の拙著 “The final works of Rich Pelz” に収録されている。